Journal Pre-proof

Primary structure determination and physicochemical characterization of DSP-3, a phosphatidylcholine binding glycoprotein of donkey seminal plasma

Sk Alim, Mikko Laitaoja, Sonali Pawar, Thirumala Rao Talluri, Janne Jänis, Musti J. Swamy

Please cite this article as: S. Alim, M. Laitaoja, S. Pawar, et al., Primary structure determination and physicochemical characterization of DSP-3, a phosphatidylcholine binding glycoprotein of donkey seminal plasma, *International Journal of Biological Macromolecules* (2023), https://doi.org/10.1016/j.ijbiomac.2023.124229

This is a PDF file of an article that has undergone enhancements after acceptance, such as the addition of a cover page and metadata, and formatting for readability, but it is not yet the definitive version of record. This version will undergo additional copyediting, typesetting and review before it is published in its final form, but we are providing this version to give early visibility of the article. Please note that, during the production process, errors may be discovered which could affect the content, and all legal disclaimers that apply to the journal pertain.

Primary structure determination and physicochemical characterization of DSP-3, a phosphatidylcholine binding glycoprotein of donkey seminal plasma

Sk Alim[1], Mikko Laitaoja[2], Sonali Pawar[1], Thirumala Rao Talluri[3], Janne Jänis[2], Musti J. Swamy[1,*]

[1]School of Chemistry, University of Hyderabad, Hyderabad-500046, India

[2]Department of Chemistry, University of Eastern Finland, FI-80101 Joensuu, Finland

[3]Equine Production Campus, ICAR-NRC on Equines, Bikaner-334001, Rajasthan, India

Running title: Primary structure and functional characterization of donkey protein, DSP-3

_____

*To whom corresponding should be addressed: School of Chemistry, University of Hyderabad, Hyderabad - 500 046, India, Tel: +91-40-2313-4807, Fax: +91-40-2301-2460, E-mail: mjswamy@uohyd.ac.in, mjswamy1@gmail.com, Website: http://chemistry.uohyd.ac.in/~mjs/

ABSTRACT

Major proteins of the seminal plasma in a variety of mammals such as bovine PDC-109, equine HSP-1/2, and donkey DSP-1 contain fibronectin type-II (FnII) domains and are referred to as FnII family proteins. To further our understanding on these proteins, we carried out detailed studies on DSP-3, another FnII protein of donkey seminal plasma. High-resolution mass-spectrometric studies revealed that DSP-3 contains 106 amino acid residues and is heterogeneously glycosylated with multiple acetylations on the glycans. Interestingly, DSP-3 exhibits significantly higher homology to HSP-1 (104 identical residues) than DSP-1 (72 identical residues). Circular dichroism (CD) spectroscopic and differential scanning calorimetric (DSC) studies showed that DSP-3 unfolds at ~45°C and binding of phosphorylcholine (PrC) – the head group moiety of choline phospholipids – increases the thermal stability. Analysis of DSC data suggested that unlike PDC-109 and DSP-1, which exist as mixtures of polydisperse oligomers DSP-3 most likely exists as a monomer. Ligand binding studies monitoring changes in protein intrinsic fluorescence indicated that DSP-3 binds lyso-phosphatidylcholine ($K_a = 1.08 \times 10^5$ M^{-1}) with ~80-fold higher affinity than PrC ($K_a = 1.39 \times 10^3$ M^{-1}). Binding of DSP-3 to erythrocytes leads to membrane perturbation, suggesting that its binding to sperm plasma membrane could be physiologically significant.

Keywords: Differential scanning calorimetry; Fibronectin type-II protein; Mass spectrometry

1. INTRODUCTION

During fertilization in mammals, seminal plasma carries spermatozoa from the male to the female uterus where it fuses with the egg, resulting in the formation zygote and fertilization. In this process, proteins of the seminal plasma play important roles in various stages of fertilization, viz. sperm capacitation, sperm-zona pellucida interaction and establishment of oviductal reservoir [1-7]. A major fraction of the proteins present in the mammalian seminal plasma have a common characteristic structure, which comprises of an *N*-terminal flanking region, followed by two or four tandemly repeating FnII domains, and show high binding specificity towards choline phospholipids [8-13]. In the last few decades, detailed studies have been carried out with seminal FnII proteins, especially the major proteins from bovine seminal plasma, PDC-109 (a mixture of non-glycosylated BSP-1 and glycosylated BSP-2) and equine seminal plasma, HSP-1/2. Results on its interaction with phospholipids indicate that PDC-109 exhibits high specificity for choline phospholipids such as phosphatidylcholine (PC) and sphingomyelin, as compared to other phospholipids such as phosphatidylglycerol, phosphatidylserine, phosphatidylethanolamine, etc. [10,11]. Moreover, the presence of cholesterol in the membranes was found to potentiate the interaction of PDC-109 with different phospholipids, which could be due to PC mediated interaction of cholesterol with the protein or its direct interaction with a putative CRAC domain in the protein [14-16]. Studies on PDC-109/*O*-phosphorylcholine (PrC) complex using single crystal X-ray diffraction showed that each PDC-109 molecule has two PC binding sites and both the binding sites are on the same face of the protein [17,18]. The major protein from equine seminal plasma, HSP-1/2, which is homologous to PDC-109, is a non-separable mixture of HSP-1 and HSP-2, which have nearly identical primary structures but differ in the number of residues in the N-terminal segment and in the extent of glycosylation [19-21].

Interaction of PDC-109 and HSP-1/2 with choline-containing ligands, model membranes and sperm plasma membranes has been greatly characterized due to the physiological significance of these proteins with choline phospholipids [22-24]. Various studies indicates that both these proteins are able to intercalate into lipid membranes and perturb the lipid chain dynamics [11,12,25-27]. Studies on membrane perturbation by PDC-109, HSP-1/2 and DSP-1 using erythrocyte cells and model membranes indicate that these proteins are able to destabilize them [28-30].

Recently, it has been observed that PDC-109 and HSP-1/2 exhibit chaperone-like activity (CLA) by protecting various target proteins against thermal, chemical and oxidative stress and hence can act as small heat shock proteins (sHsps) [29, 31-33]. It was also found that the CLA is modulated by a variety of factors including oligomeric status of the protein and its hydrophobicity, ligand/membrane binding, pH and ionic strength and that the membrane destabilizing activity and the CLA of these proteins are inversely correlated by a 'pH switch' [29,31-35]. Mutational studies indicated that conserved core tryptophan residues of FnII domains are essential for the membrane-perturbing and chaperone-like activities of PDC-109 [36]. In other studies it was found that glycosylation differentially modulates the membrane-perturbing and chaperone-like activities of PDC-109, with the glycosylated protein expressing higher CLA whereas the non-glycosylated protein exhibited higher membrane perturbing activity [37].

From the above it can be seen that the major FnII proteins of mammalian seminal plasma play very important roles in priming spermatozoa for fertilization as well as in protecting other seminal plasma proteins from inactivation or misfolding as exemplified by PDC-109 and HSP-1/2. Therefore, it is important to purify the major FnII proteins from others mammal seminal plasma and characterize them in detail and to develop structure-function relationships among them. Such studies are likely to lead to a better understanding

of the functional roles played by them. In this direction, in a recent study we have purified three choline binding proteins from donkey seminal plasma (DSP-1, DSP-2 and DSP-3) and characterized the macromolecular properties of DSP-1 in detail [30,38]. The main objective of the present study is to characterize DSP-3 using biochemical and biophysical methods in order to obtain information on its structural characteristics and functional properties. The results of high-resolution mass spectrometric studies yielded the primary structure of DSP-3 and showed that DSP-3 belongs to the seminal FnII family. Circular dichroism (CD) spectroscopic and computational modelling studies yielded information on the secondary and tertiary structures of this protein. In addition, we also investigated the thermal stability of DSP-3 and characterized the binding of PrC and lyso-phosphatidylcholine (Lyso-PC) to it. The results indicate that DSP-3 exhibits membrane destabilizing activity against model cell membranes and that the thermal unfolding temperature of DSP-3 increases significantly upon PrC/Lyso-PC binding. These observations suggest that DSP-3 may play a physiologically important role in fertilization.

2. MATERIALS AND METHODS

2.1. Materials

Phosphorylcholine chloride (calcium salt) and heparin-agarose type-I affinity matrix were obtained from Sigma (St. Louis, MO, USA). *p*-Aminophenyl phosphorylcholine-agarose column was purchased from Pierce Chemicals (Oakville, Ontario, Canada). DMPC and Lyso-PC from egg yolk were obtained from Avanti Polar Lipids (Alabaster, AL, USA). All other chemicals were purchased from local suppliers.

2.2. Purification of DSP-3

In a previous report we described the purification of DSP-1, DSP-2 and DSP-3, the three most abundant proteins in the donkey seminal plasma, using a modified procedure reported

previously for HSP-1/2 [31,32]. The procedure involves affinity chromatography on heparin-agarose and *p*-aminophenyl phosphorylcholine-agarose (PPC-agarose), followed by RP-HPLC (Fig. S1) [30,32]. Additional details are given in the supplementary information. The purified DSP-3 thus obtained was dialyzed against 50 mM Tris/HCl buffer containing 150 mM NaCl and 5 mM EDTA, pH 7.4 (TBS) and stored at 4 °C. Homogeneity of the purified protein was assessed by SDS-PAGE [39]. All experiments on DSP-3 were performed in TBS unless specified otherwise.

2.3. Mass spectrometry

Mass spectrometric characterization of DSP-3 was done using a protocol similar to that employed earlier for DSP-1 [30]. Briefly, protein samples were buffer-exchanged to 20 mM ammonium acetate (pH 7.4) using PD-10 desalting columns (Cytiva Europe GmbH). Additional purification was done using size-exclusion chromatography (SEC) on Äktapurifier 100 instrument (Amersham Pharmacia Biotech AB, Uppsala, Sweden), using a Superdex 75 column (GE Life Sciences, Sweden). Trypsin digestion was performed by incubating the protein samples overnight with sequencing grade trypsin (Sigma Aldrich, USA) at a 1:50 (w/w) trypsin-to-protein ratio using a mixture of acetonitrile (MeCN)/water (1:1, v/v) containing 10 mM dithiothreitol (DTT) as the solvent. The intact protein samples and their tryptic digests were analysed using an HPLC system (UltiMate 3000; Thermo Scientific) connected to a 12-tesla FT-ICR mass spectrometer (Bruker solariX XR; Bruker Daltonics, Germany). The proteins/peptides were eluted over an Acclaim Pepmap100 C18 (0.075×150 mm, 3 µm) column (Thermo Scientific) at a flow rate of 0.5 µL/min, using a solvent gradient of 1–40% acetonitrile with 0.2% formic acid. Fragmentation of the peptides was performed with collision induced dissociation (CID) measurements using argon as the collision gas and previously optimized voltages. Direct infusion top-down MS/MS experiments were performed on a QTOF mass spectrometer (Bruker timsTOF; Bruker Daltonics, Germany).

6

The instruments were controlled and the data were acquired using Chromeleon 6.80 (UltiMate 3000), ftmsControl 2.0 (solariX) or otofControl 5.1 (timsTOF) software, respectively. Post-processing of the data and further analysis were accomplished by using Bruker DataAnalysis 5.1 software.

2.4. Circular dichroism spectroscopy

CD spectroscopic studies were performed using an AVIV model 420SF CD spectrometer (Lakewood, NJ, USA) fitted with a thermostatic cell holder and a thermostatic water bath at a scan speed 20 nm/min. Far- and near-UV CD spectra were recorded using a 0.2 cm path length quartz cell with samples containing DSP-3 at a concentration of 0.1 mg/mL and 0.5 mg/mL, respectively, in 10 mM Tris/HCl buffer, pH 7.4. Each spectrum recorded was the average of 6 consecutive scans from which buffer scans were subtracted. Spectra were also obtained in the presence of 20 mM PrC.

Thermal unfolding of DSP-3 was investigated by monitoring the CD spectral intensity of the protein (0.1 mg/mL) at 224 nm and the temperature was increased from 25 to 80 °C at a scan speed 1°/min. The effect of binding of different ligands such as PrC, Lyso-PC or DMPC, binding on the thermal stability of DSP-3 was investigated by incubating 0.1 mg/mL protein for ~30 min with 50 mM PrC, or 100 µM DMPC or 100 µM Lyso-PC before the temperature scans were performed.

2.5. Computational modelling

The amino acid sequence of DSP-3 determined by mass spectrometry was submitted to I-TASSER server (http://zhanglab.dcmb.med.umich.edu/I-TASSER) to build a 3-dimensional structural model of the protein. The crystal structure of PDC-109 (pdb code: 1H8P) was used as a scaffold template. In addition, binding of PrC to the two FnII domains of DSP-3 was also studied *in silico* using the I-TASSER server.

2.6. Differential scanning calorimetry (DSC)

DSC measurements were performed using a Nano DSC equipment from TA instruments (New Castle, Delaware, USA) described earlier [40]. DSP-3 (0.5 mg/mL) in TBS was heated from 20 to 80 °C at a scan rate of 1 °C/min under a constant pressure of 3.0 atmosphere. Buffer base line scan was subtracted from all the sample data to eliminate the contribution from buffer to the calorimetrically measured heat capacity of the protein. To investigate the effect of PrC binding, DSP-3 was pre-incubated with different concentrations of PrC and experiments were carried out under similar conditions and the thermograms were analysed using the 'Gaussian Model' in the DSC data analysis software provided by the instrument manufacturer.

2.7. Steady-state fluorescence studies

Steady state fluorescence measurements were performed using a JASCO PF-850 fluorescence spectrometer at room temperature, with both excitation and emission band pass filters set at 3 nm. All experiments were carried out with samples taken in a $1\times 1\times 4.5$ cm quartz fluorescence cuvette. DSP-3 ($OD_{280} < 0.1$) in TBS was excited at 280 nm and emission spectra were recorded between 300 and 420 nm. Ligand binding experiments were performed by adding various lipids at mentioned concentrations to DSP-3 and the spectra were recorded after 3 min of incubation. Titrations to determine the association constants for ligand binding were carried out by adding small aliquots of the ligand from a concentrated stock solution (100 μM Lyso-PC, or 20 mM PrC) in TBS to DSP-3 (~0.1 OD) taken in the same buffer. Egg yolk Lyso-PC will be mostly in the micellar form under these conditions.

2.8. Erythrocyte lysis assay

Erythrocyte lysis assay to assess the ability of DSP-3 to perturb the cell membrane was performed as described earlier [28,29]. In order to investigate the concentration dependence of the protein on cell lysis, 100 μL of 4% human erythrocytes in TBS were incubated with different concentrations of DSP-3 and the final volume was adjusted to 0.5 mL with TBS.

8

After incubating the mixture for 1 h at room temperature, the sample was centrifuged at 3000 rpm for 10 min. The supernatant was collected and optical density was checked at 415 nm, which corresponds to absorption of the haem moiety, using a Shimadzu UV-3600 UV-Vis NIR spectrophotometer. For investigating the kinetics of erythrocyte membrane disruption, 150 µg/mL of DSP-3 was incubated with 100 µL of 4% RBC suspension in different vials and incubated for different time intervals (5-300 min) before measuring absorbance as described above. To investigate the effect of ligands on erythrocyte membrane disruption, DSP-3 was pre-incubated with PrC, Lyso-PC and choline chloride (ChCl) prior to its addition to the erythrocyte suspension, and the experiment was carried out as described above. Results from a minimum of three independent experiments have been presented along with standard deviations.

2.9. Microscopy

Images of human erythrocytes in the presence of DSP-3 were obtained using a LSM 880 confocal microscope (Jena, Germany) as described earlier [29,30]. To investigate the effect of DSP-3 on the cell morphology and membrane integrity, a 0.04% suspension of human erythrocytes in TBS was incubated with 150 µg/mL of protein. After incubation, 50 µL aliquots of the mixture were taken at 60 min and 90 min, spotted on a clean glass slip (Thermo Fisher) and shifted to confocal stage for imaging. The erythrocyte suspension in TBS alone was used as the control. To investigate the effect of ligand binding, DSP-3 was pre-incubated with 20 mM PrC, or 20 µM Lyso-PC or 20 mM ChCl for 10 min before its addition to the erythrocyte suspension.

2.10. Preparation of liposomes

Lipids taken in a glass tube were dissolved in either dichloromethane or dichloromethane-methanol mixture (2:1, v/v) and were dried under a gentle stream of nitrogen gas and then by vacuum desiccation for 3-4 h [38]. The lipid film was hydrated with buffer to give the desired

lipid stock concentration. Small unilamellar vesicles (SUVs) were prepared by homogenizing the lipid mixture with 3-4 freeze-thaw cycles followed by sonication of the lipid suspension for 30 min in a bath sonicator above their transition temperature.
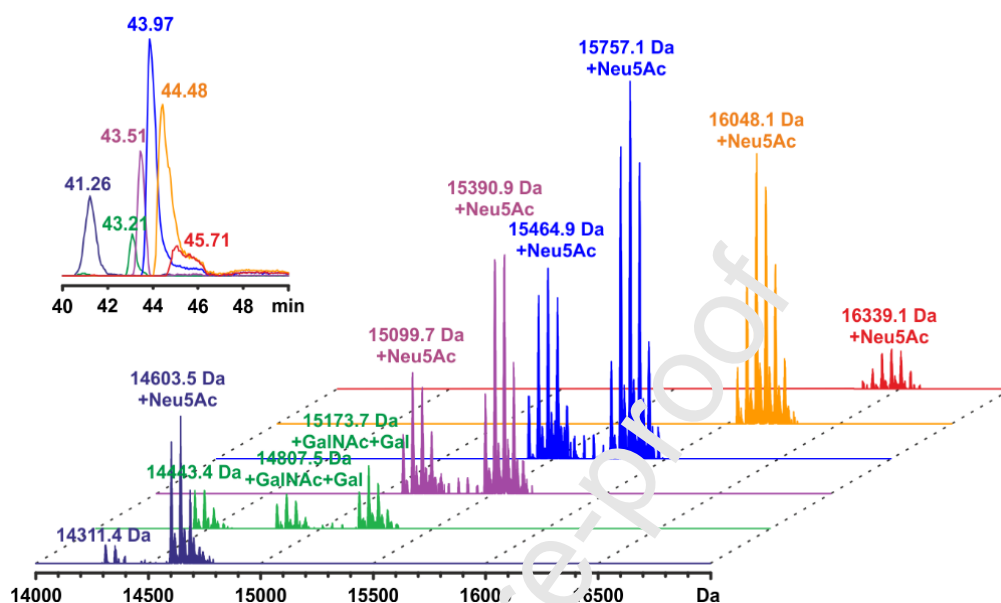
Figure 1. LC ESI FT-ICR mass analysis of DSP-3. Deconvoluted mass spectra of different glycoforms of DSP-3, eluting at around 41.26, 43.21, 43.51, 43.97, 44.48, and 45.71 min are shown. The inset shows the corresponding extracted ion chromatograms (for the total ion chromatogram, see Supporting Information). Color code used in the mass spectra connects the glycoforms to the peaks in the inset. The peak patterns for each glycoform are due to multiple protein acetylations (+42 Da). The most abundant isotopic masses are given for the non-acetylated proteoforms of the each detected glycoform.

3. RESULTS AND DISCUSSION

3.1. Primary structure of DSP-3

LC-MS measurements showed that DSP-3 is expressed as a heterogeneous mixture of different proteoforms (Fig. 1, Fig. S2), which is similar to that observed with DSP-1 [30]. The observed intact masses for DSP-3 were around 14.3 to 16.3 kDa, which are somewhat smaller than for DSP-1 [30]. In addition, similar peak patterns originating from multiple acetylations (+42 Da) were observed for each detected DSP-3 glycoform. Trypsin digestion

10

and the subsequent LC-MS/MS analysis was only able to partially determine the sequence of the DSP-3 with peptides best matching to those predicted for *Equus asinus* mRNA sequence of 014723760.1, which was used as a model template when assigning the peptides. Thereby, the primary structure of DSP-3 was found to be similar to the other seminal plasma proteins (Fig. 2). As in the case of DSP-1, the N-terminal part of the sequence was determined by top-down MS/MS experiments [30]. The disulfides were not reduced to limit the fragmentation to the N-terminal part only. The intact protein ions at *m/z* ~1500 were isolated and fragmented at a collision energy of 60 eV. This resulted mainly in small fragments corresponding to the released glycans (Fig. S3) as well as large protein ions (~12 kDa) with a complete removal of glycans. The glycan fragmentation showed small N-acetylgalactosamine (GalNAc) and galactose (Gal) containing fragments, further modified by sialic acid (Neu5Ac) or acetylated sialic acid (Neu5,xAc$_2$) residues. These structures indicate that there are multiple O-glycosylation sites in the N-terminal part of DSP-3, similar to some of the other seminal plasma proteins [20,41,42]. For the large protein ions observed, the smallest fragment had a mass of 12456.62 Da, which corresponds to the full amino acid chain of DSP-3 without attached glycans. When the collision energy was increased to 70 eV, additional fragments from the N-terminal part were observed which allowed a partial sequencing of the N-terminal region. The determined sequence showed a partial match with the recently updated *Equus asinus* mRNA sequence (044614940.1). It is likely that the genes and intron/exon use of *Equus hemionus* is different from that of *Equus asinus.* By considering some variations in the amino acid sequence, one tryptic peptide could be associated with this region to ultimately discover the complete sequence of DSP-3. The mass calculated from the amino acid sequence of DSP-3, without the associated glycans, is 12456.66 Da, which perfectly matches with the experimental mass obtained from the top-down MS measurements.

predicted signal peptide

MAPRLGIFLILAGTCIFLQLDHVDG–

N-terminal extension   1 FnII

DKQPITTTLSATMKTDNQCVFPFDYSGKRYFQCTRTGSFHRWCSLTENYSGKWRYC

MS/MS sequencing   1775.7944

1971.8902
1699.7433
2157.9708

linker   2 FnII

VAEDYAKCFFPFVYRGRTYHTCTTDGSFFLIPWCSVTPNYDRDGGWKYCM

1402.6340   1562.7580
2732.2698   4076.7847
2117.9444   3879.6526
2462.1391   2923.2954
2119.9587   2921.2768
1060.4531   3861.64
1674.7823   3 3.6 79

Figure 2. The complete amino acid sequence of DSP-3 with the identified tryptic peptides and their monoisotopic masses indicated. The disulfide linkages shown are based on the similarity with the other homologous mammalian seminal FnII proteins, PDC-109 and HSP-1/2. The N-terminal extension part is most likely missing due to the observed protein modifications (glycosylations/acetylations) and was characterized by additional top-down MS experiments.

Comparison of the primary structure of DSP-3 with that of a number of FnII proteins isolated from the seminal plasma of several other mammals, namely bull, horse, pig, mouse, donkey and human, employing multiple sequence alignment is given in Fig. 3. This comparison shows that when DSP-1 equine seminal plasma protein, HSP-1 are compared, only 2 residues are different. On the other hand, a comparison of DSP-1 and DSP-3 showed that only 72 residues are exactly identical, whereas next best match is found with BSP-A3, with 53 residues matching with BSP-A3 (second highest). Thus, it is interesting that DSP-3 differs considerably with all other seminal FnII proteins. However, importantly all 8 Cys residues that form the characteristic disulfide bonds in the two FnII domains are conserved

among all the proteins. In addition, all the 4 core tryptophan residues which have been shown to be important for the choline phospholipid binding and chaperone-like activities of PDC-109 [36], are conserved in all the above proteins.
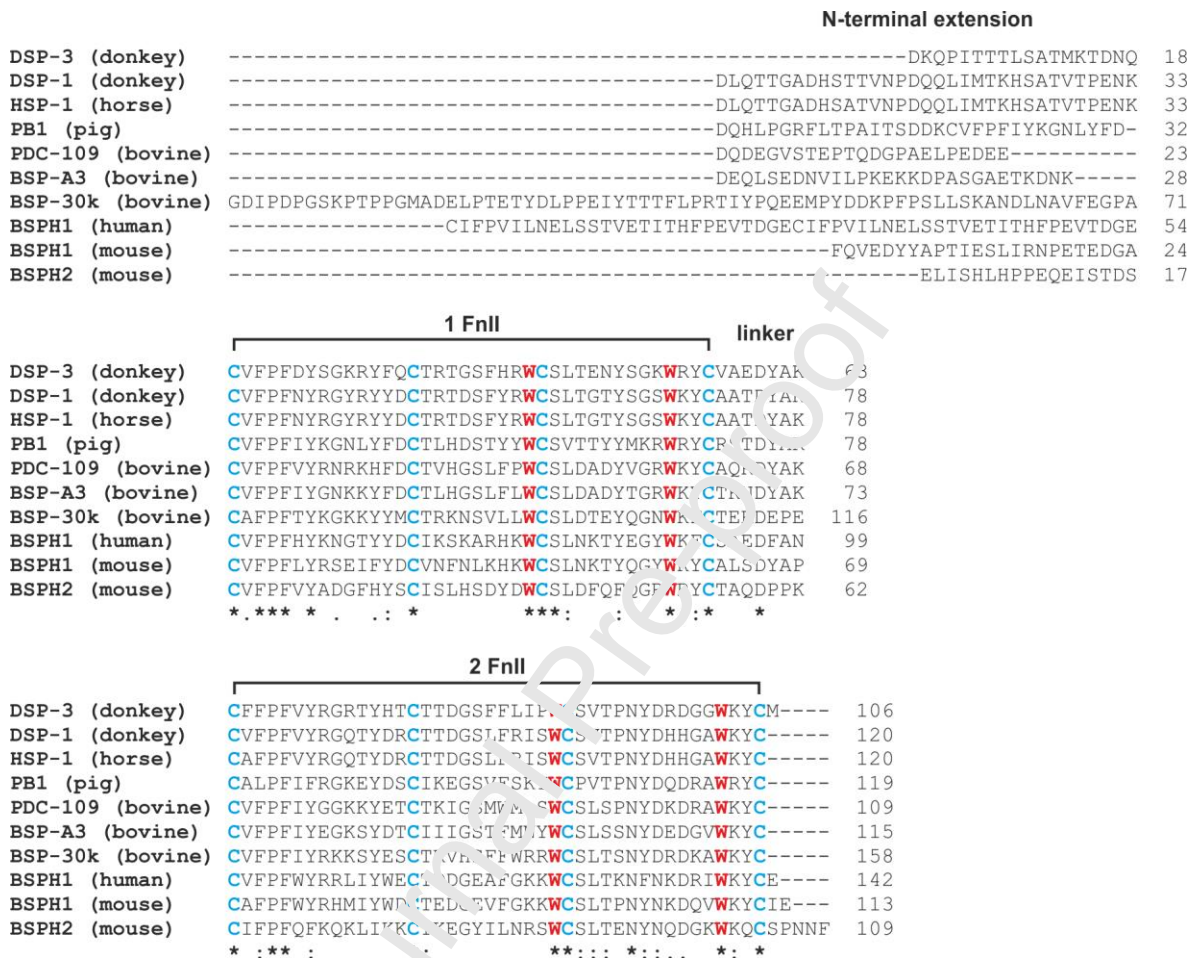
Figure 3. Multiple sequence alignment of the primary structure of DSP-3 with seminal plasma FnII proteins of various mammals. Only proteins containing 2 FnII domains have been selected. All sequences were taken from EMBL-EBI database and aligned using Clustal Omega program (https://www.ebi.ac.uk/Tools/msa/clustalo/) without signal peptide sequences. The proteins (with database IDs in parentheses) are: HSP-1 (SP:P81121); porcine (pig) seminal plasma protein, PB1 (SP:P80964); bovine seminal plasma proteins PDC-109 (SP:P02784), BSP-A3 (SP:P04557) and BSP-30k (SP:P81019); human seminal plasma protein, BSPH1 (SP:Q075Z2); mouse seminal plasma proteins, BSPH1 (SP:Q3UW26) and BSPH2 (SP:Q0Q236). Conserved cysteine residues involved in disulfide bonds are shown in bold cyan, conserved core tryptophans are shown in bold red. Residues that are fully conserved across all species (*) and residues that are similar (: and .) are indicated.
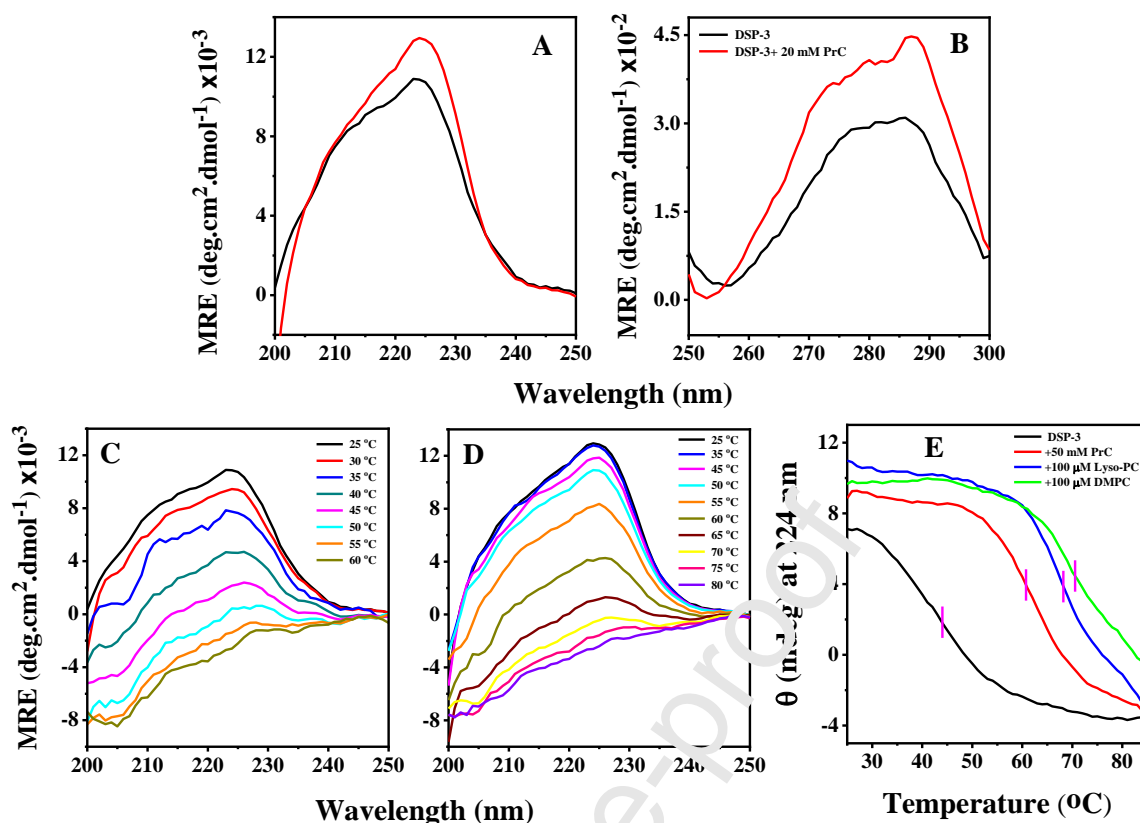
Figure 4. Circular dichroism spectroscopic studies of DSP-3. (**A**, **B**) Far- and near-UV CD spectra, respectively, of DSP-3 alone (black) and in the presence of 20 mM PrC (red). (**C**, **D**) Far-UV CD spectra of DSP-3 in the absence and presence of 20 mM PrC, respectively, recorded at different temperatures. (**E**) Effect of different ligands on the thermal stability of DSP-3. Thermal scans were obtained by recording the CD signal intensity of the protein at 224 nm as the temperature was increased at a scan rate of 1°/min. A fixed concentration of protein (0.1 mg/mL) was incubated with different ligands. Black, DSP-3 alone; red, + 50 mM PrC, blue, + 100 μM Lyso-PC; green, + 100 μM DMPC.

3.2. Secondary and tertiary structure of DSP-3

The secondary and tertiary structures of DSP-3 were characterized by CD spectroscopy. Far-UV CD spectra of DSP-3 alone and in the presence of 20 mM PrC – the head group moiety of its physiological ligand, phosphatidylcholine – are shown in Fig. 4A. The far-UV CD spectrum of DSP-3 alone (black) is characterized by a broad positive asymmetric band with its maximum at 224 nm and a couple of shoulders at ~216 nm and 210 nm. In the presence of 20 mM PrC, the spectral intensity at 224 nm increases, whereas the spectral intensity

14

decreases slightly below 205 nm (red). The near-UV CD spectrum of DSP-3 is quite broad, possibly due to the presence of several overlapping bands with maxima in the 275-290 nm region, and exhibits a maximum at ~286 nm (Fig. 4B). In the presence of 20 mM PrC, the spectral intensity increases significantly and exhibits a more distinct maximum at ~287 nm, although the overall spectrum is quite broad indicating the presence of several underlying, overlapping bands. Further, in the presence of 20 μM Lyso-PC (micelles) and 20 μM DMPC (liposomes) the spectral intensity increases in both the cases, although no major changes are observed in the shape of the spectrum (Fig. S4). The positive band in far-UV CD spectrum of DSP-3 could not be analysed to obtain the secondary structural elements of the protein, due to lack of suitable reference dataset, as was the case with the other major mammalian seminal plasma proteins, namely PDC-109, HSP-1/2 and DSP-1 [30,32,43].

Far- UV CD spectra of DSP-3 recorded at various temperatures between 25 and 60 °C show a gradual decrease in the spectral intensity with increase in temperature, suggesting a gradual loss of the secondary structure of the protein (Fig. 4C). Broadly similar changes can be seen in the near UV CD spectra (Fig. S5A). In contrast, in the presence of 20 mM PrC only moderate changes are seen in the far- as well as near-UV CD spectra between 25 and 50 °C, whereas significant decrease in signal intensity was observed with further increase in temperature in the range of 55-70 °C (Fig. 4D, Fig. S5B). Further increase in temperature led to only moderate changes in the spectral intensity. The thermal stability of DSP-3 and the effect of ligand binding were also investigated by monitoring the CD signal intensity of the protein at 224 nm while the temperature is continuously varied. CD thermal scans recorded in the absence and presence of different ligands, viz., PrC, Lyso-PC and DMPC are shown in Fig. 4E. The signal intensity of native DSP-3 decreases with the steepest decline being seen at ~45 °C, which is taken as the midpoint of thermal unfolding of the protein. In the presence

of 50 mM PrC the midpoint of unfolding shifted to ~61 °C, whereas in the presence of 100 μM concentrations of Lyso-PC and DMPC it shifted to ~68 °C and ~70 °C, respectively.
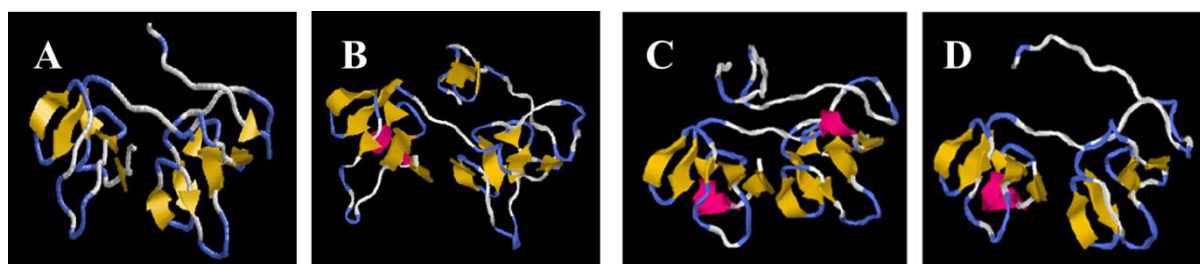

Figure 5. Three dimensional structural models of DSP-3 (A) DSP-1 (B), HSP-1 (C) and PDC-109 (D). The structures were generated by computational modelling using the I-TASSER program available online (http://zhanglab.dcmb.med.umich.edu/I-TASSER) using the reported crystal structure of PDC-109 (pdb code: 1h8p) as the template. The models of DSP-1, HSP-1 and PDC-109, taken from our previous work [30,32], are shown here for comparison.

3.3. Computational modelling of DSP-3 structure and binding of PrC

As the secondary structure of DSP-3 could not be determined from the near-UV CD spectra, we used computational methods to obtain 3-dimensional structural model of DSP-3 using Iterative Threading ASSEmbly Refinement (I-TASSER) program (http://zhanglab.dcmb.med.umich.edu/I-TASSER) using the reported crystal structure of PDC-109 (pdb code: 1h8p) as the template. The modeled structure of DSP-3 is shown in Fig. 5 together with the modeled structures of DSP-1, HSP-1 and PDC-109, taken from our earlier studies on DSP-1 and HSP-1/2 [30,32]. A careful observation of the models indicates that the overall structure of DSP-3 is very similar to those of PDC-109, HSP-1 and DSP-1. Further, the relative content of various secondary structures of the three proteins, deduced from the computational models are rather similar, with all three proteins containing very little α-helix and about 20-25% β-sheet, whereas ~70% of the residues are in β-turns and unordered structures (Table 1).

16

Table 1. Secondary structure of DSP-3, DSP-1, HSP-1 and PDC-109 estimated from computational modelling using the I-TASSER server. Secondary structure data of PDC-109 deduced from its crystal structure (pdb code: 1h8p) is also given for comparison.

Protein	α-helix	β-sheet	β-turns + unordered structures
DSP-3	-	20.8	79.2
DSP-1	3.3	25.0	71.7
HSP-1	5.8	25.0	69.1
PDC-109 (from modelling)	3.7	23.8	72.4
PDC-109 (from crystal structure)	9.2	22.9	67.8
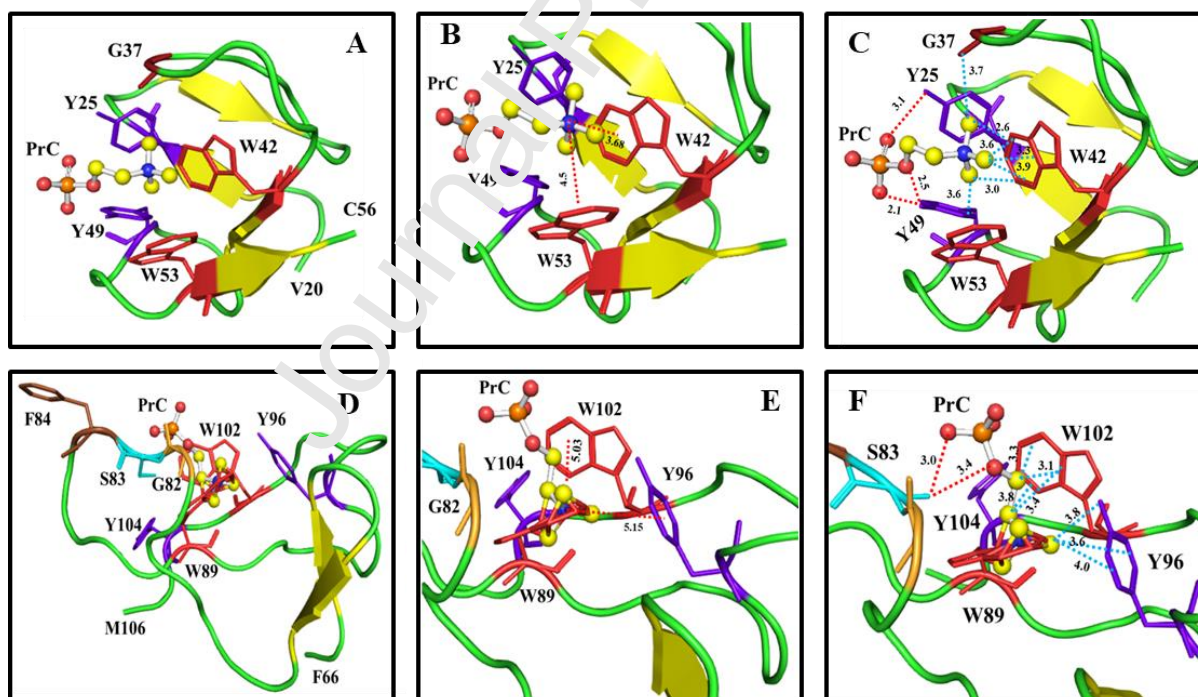
Figure 6. Structure of the FnII domains of DSP-3 with bound PrC, generated using I-TASSER. The structures have been visualized using PyMOL. The side chains of binding site residues are shown in stick format. (**A**) Binding to FnII domain-I with interacting residues labeled. (**B**) Cation-π interaction of the quaternary ammonium group with W42 and W53 are

indicated by red dotted lines. (**C**) Hydrogen bonds between the hydroxyls of Y25 and Y49 and the phosphate oxygens are shown in red dotted lines and the possible CH-π and CH-O interactions are shown as blue dotted lines. (**D**) Binding to FnII domain-II with interacting residues labeled. (**E**) The cation-π interaction of the quaternary ammonium group with W89,W102 and Y96 are indicated by red dotted lines. (**F**) Hydrogen bonds between the hydroxyls of S98 and the phosphate oxygen are shown as red dotted lines and the possible CH-π and CH-O interactions are as blue dotted lines.

Along with building a 3-D model of DSP-3 we also investigated the binding of PrC to its FnII domains using the I-TASSER server. The structures of DSP-3 domain-I and domain-II with bound PrC molecules are shown in Fig. 6A and 6D, respectively. PrC binding to DSP-3 is mediated by multiple weak interactions including cation-π, O-H···O and C-H···O hydrogen bonds as well as C-H···π interactions. Besides the classical hydrogen bonds where N-H and O-H groups form weak interactions with O and N atoms of other groups, recent work has demonstrated that C-H···O, cation π and C-H···π interactions also stabilize protein structure and protein-ligand interactions [44-46]. The cation-π interactions in the two FnII domains are shown in Figs. 6B and 6E whereas the H-bonding and C-H···π interactions are shown in Figures 6C and 6F. It is observed that in first FnII domain of DSP-3, 4 out of the 5 residues that interact with PrC, namely Y25, Y49, W42 and W53 are fully conserved, whereas G37 is highly conserved among the FnII proteins whose sequences are used for comparison in the multiple sequence alignment shown in Fig. 3. Similarly, in the second FnII domain, W89, W102 and Y96 which interact with PrC are fully conserved whereas S83 which forms an important O-H O hydrogen bond with PrC is conserved among 6 out of 9 sequences.
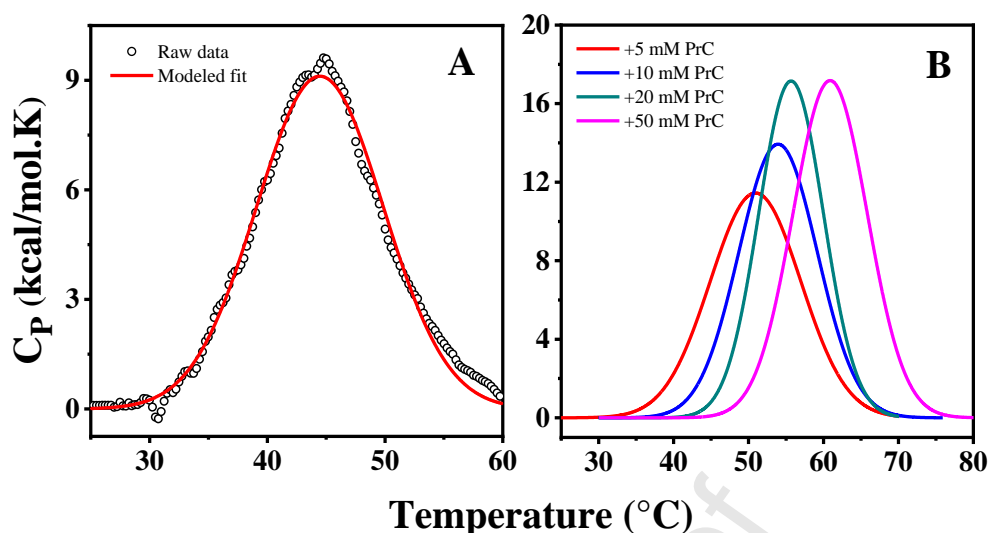
Figure 7. Thermal unfolding of DSP-3. (**A**) DSC thermogram of native DSP-3. Open circles correspond to the experimental data and the red line corresponds to a fit of the experimental to the Gaussian model. (**B**) Thermograms of DSP-3 in the presence of different concentration of PrC: 5 mM (red), 10 mM (blue), 20 mM (dark cyan) and 50 mM (magenta).

3.4. Thermal denaturation of DSP-3 and the effect of ligand binding

DSC studies were performed to investigate the thermal unfolding of DSP-3 in more detail as well as to obtain the thermodynamic parameters associated with it. Thermograms of DSP-3 alone and in the presence of different concentrations of PrC are shown in Fig. 7A and 7B, respectively. The thermogram of native DSP-3 show a single thermotropic transition centred at ~44.5 °C (Fig. 7A). In comparison, DSP-1 showed two thermotropic transitions centred at ~32 and 43 °C, which were assigned to dissociation of oligomers and unfolding of the monomer (Alim et al., 2022) [30]. The absence of the minor transition before the major transition and the excellent fit of the endothermic peak in the thermogram to a single component indicate that DSP-3 exists as a monomer in solution. Further, this observation also indicates that the thermal unfolding of DSP-3 is a two-state transition, wherein the protein goes from a fully folded form to a completely unfolded state. A possible physiological implication of the monomeric state of DSP-3 is that it most likely exhibits little or no chaperone-like activity unlike the other well-characterized seminal FnII proteins such as

19

PDC-109, HSP-1/2, whose CLA has been correlated to their oligomeric structure. However, this needs to be verified experimentally and we propose to carry out such studies with DSP-3 in the near future.

The transition temperature determined from the DSC is also in excellent agreement with that estimated from CD thermal scans, which showed a steep decrease in the spectral intensity at 224 nm at 45 °C. Further, in the presence of PrC, the temperature and enthalpy associated with the unfolding transition of DSP-3 shift to higher values with increase in the concentration of the ligand (Fig.7B, Table S2). These observations are similar to those made with DSP-1 and PDC-109 [30,43]. The thermotropic transition temperature of DSP-3 shifted from 44.5 °C in the absence of PrC to ~60.9 °C in the presence of 50 mM PrC, with a concomitant increase in the transition enthalpy from 125 kJ/mol to 213 kJ/mol. These results strongly suggest that PrC binding stabilizes the structure of DSP-3, resulting in an increase in its unfolding temperature.
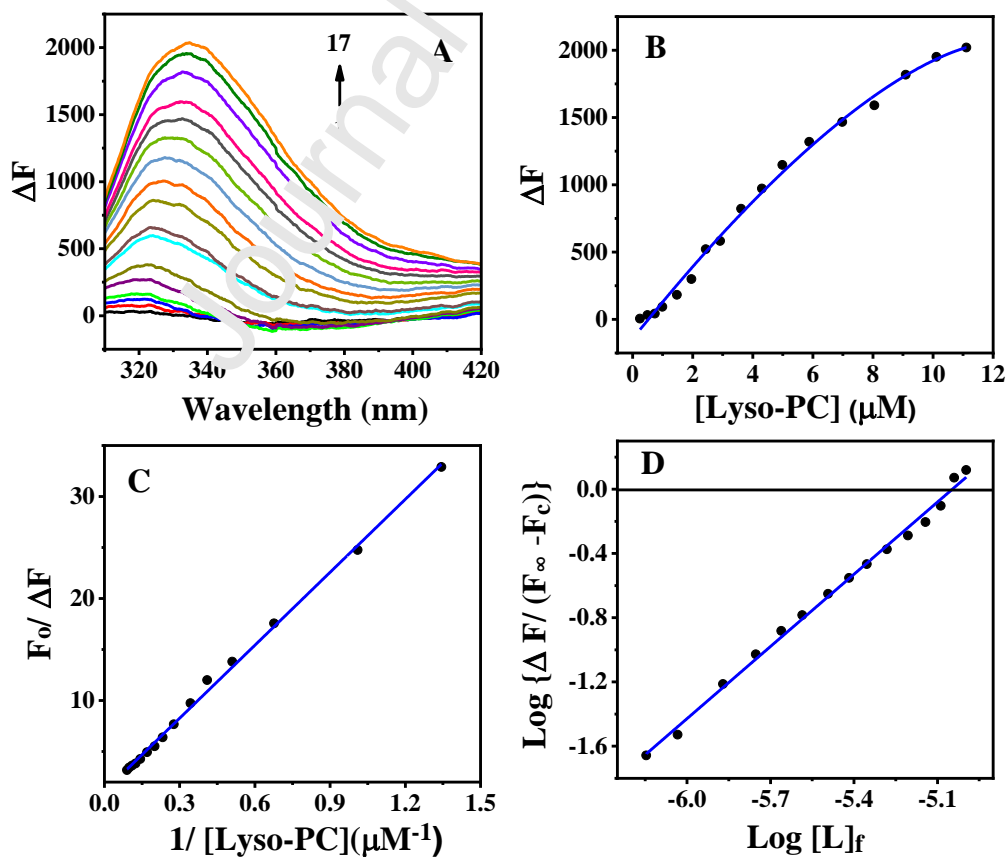
Figure 8. Fluorescence titration to determine the association constant, K_a for Lyso-PC binding to DSP-3. (**A**) Fluorescence difference spectra of DSP-3 obtained in the presence of various concentrations of Lyso-PC. (**B**) Binding curve obtained by plotting ΔF versus [Lyso-PC]. (**C**) A double reciprocal plot of $F_o/\Delta F$ versus $1/$[Lyso-PC]. From the Y-intercept of the plot F_∞, the fluorescence intensity of the protein at saturation binding is obtained. (**D**) A double log plot of [log $\{\Delta F/(F_\infty - F_c)\}$] versus log $[L]_f$. From the X-intercept of the plot the association constant, K_a for Lyso-PC binding to DSP-3 is obtained. See text for details.

3.5. Intrinsic fluorescence studies on the binding of Lyso-PC and PrC to DSP-3

The binding of PrC and Lyso-PC to DSP-3 was investigated by monitoring ligand induced changes in the intrinsic fluorescence intensity of the protein. Fluorescence spectra corresponding to the titration with Lyso-PC and PrC are given in Fig. S6A and B and plots reporting the analysis of the titration data for Lyso-PC binding are given in Fig. 8, and for the binding of PrC are given in Fig. S7. To simplify the discussion, only the data analysis corresponding to the binding of Lyso-PC will be discussed below, since analysis of the data for PrC is essentially identical. Addition of small aliquots of Lyso-PC led to incremental increases in the emission intensity of the protein (Fig. S6A) along with a small blue shift in the emission maximum and the difference spectra obtained by subtracting the spectrum of the protein alone from the spectra recorded in the presence of increasing concentrations of Lyso-PC are shown in Fig. 8A. A plot of change in fluorescence emission intensity (ΔF) at 333 nm versus the ligand concentration showed saturation behaviour (Fig. 8B).

In order to obtain the association constant K_a, the titration data was analysed by the Chipman plot as described earlier for the interaction these ligands to PDC-109 and DSP-1 [23,30]. In brief, a plot of $1/\Delta F$ versus $1/[L]_t$, yielded a straight line (Fig. 8C). Here ΔF (= $|F_c - F_o|$) refers to the change in fluorescence intensity at any point of the titration and F_o and F_c correspond to the fluorescence intensity of DSP-3 alone and in the presence of ligand, respectively, and $[L]_t$ is the corresponding total ligand concentration. From the ordinate

21

intercepts of this plot, F_∞, fluorescence intensity of the sample at infinite concentration, was calculated. The titration data was further analysed according to following expression [23,47]:

$$\text{Log } \{\Delta F/(F_\infty - F_c)\} = \text{Log } K_a + \text{Log } [L]_f \qquad (1)$$

where $[L]_f$, the free ligand concentration, is given by:

$$[L]_f = [L]_t - \{(\Delta F/\Delta F_\infty)[P]_t\} \qquad (2)$$

where $[L]_t$ and $[P]_t$ are total ligand concentration and total protein concentration, respectively, and ΔF_∞ ($= F_\infty - F_0$) is the change in fluorescence intensity at infinite concentration (at saturation binding). From the X-intercepts of plots of log $\{\Delta F/(F_\infty - F_c)\}$ versus log $[L]_f$ the association constant, K_a for the binding of Lyso-PC and PrC to DSP-3 were determined (Fig. 8D, Fig. S7D). The association constants thus obtained were 1.08 ($\pm$ 0.04) $\times$ 10^5 M^{-1} for Lyso-PC and 1.39 ($\pm$ 0.08) $\times$ 10^3 M^{-1} for PrC (averages of two independent titrations). These results show that DSP-3/Lyso-PC association is almost 80-times stronger than the DSP-3/PrC interaction.

The blue shift observed in the fluorescence emission of DSP-3 upon interaction with PrC is similar to the results obtained with PDC-109 [23]. This indicates that the microenvironment around Trp residues involved in the lipid binding becomes more hydrophobic in nature upon binding of these ligands containing choline moiety.

3.6. Spectrophotometric and microscopic studies on DSP-3 binding to erythrocytes

To investigate the effect of DSP-3 binding on the cell membrane, human erythrocytes were taken as a model cell system, as both spermatozoa and erythrocytes of different mammalian species consist of high proportion of choline phospholipids [28,48-51]. Binding of DSP-3 to erythrocytes caused the disruption of membrane structure which led to cell lysis and release of haemoglobin into the solution. This was monitored by measuring absorption at 415 nm corresponding to the haem in the released haemoglobin [28]. After incubation with DSP-3, the amount of haemoglobin released from erythrocytes increased in a sigmoidal curve and

reached saturation at ~100 μg/mL concentration of DSP-3, indicating concentration-dependent membrane destabilization (Fig. 9A). Kinetics of DSP-3 induced erythrocyte destabilization, which was monitored over time periods of 5-300 min, indicated that the release of haemoglobin increased as the incubation time was increased up to 180 min and then levelled off (Fig. 9B). These results indicate that DSP-3 binding destabilizes the erythrocyte membrane in a time- and concentration-dependent manner.
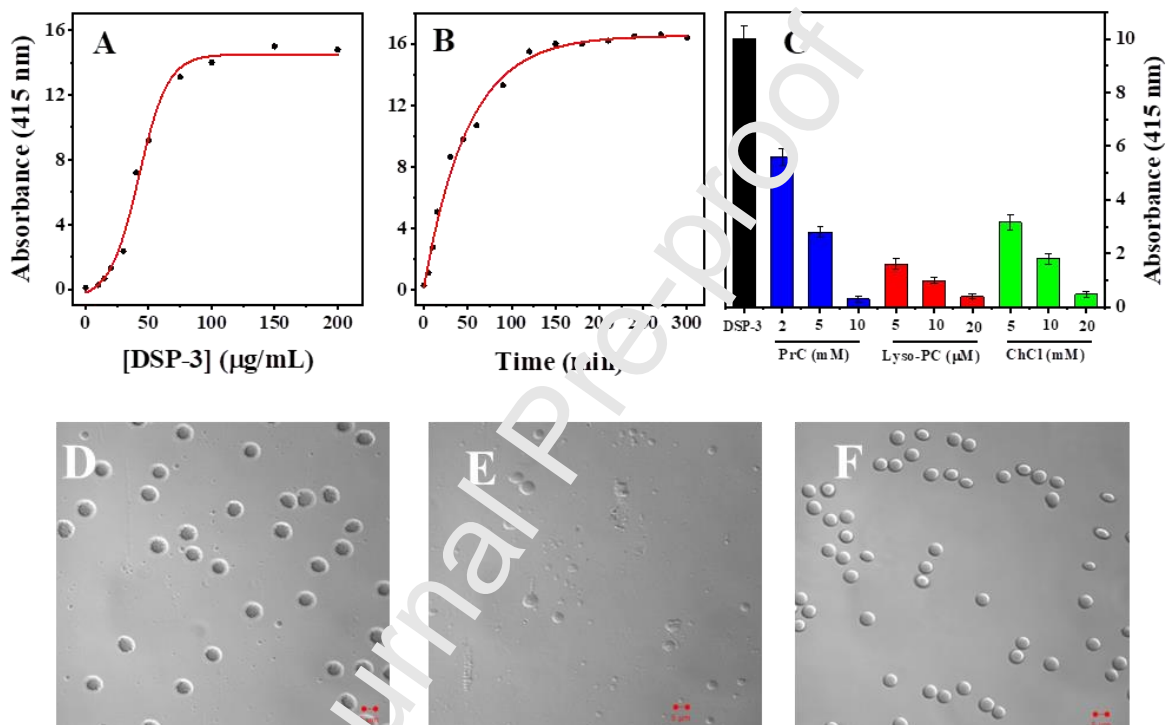
Figure 9. Effect of DSP-3 on human erythrocyte membrane. (**A**) Effect of increasing the concentration of DSP-3 on erythrocyte lysis. (**B**) Kinetics of erythrocyte lysis induced by DSP-3. The protein concentration in each sample was 100 μg/mL. (**C**) Erythrocyte lysis induced by DSP-3 alone and upon pre-incubation with different concentrations of Lyso-PC, PrC and choline chloride. Absorbance at 415 nm was measured to detect the haemoglobin released upon cell lysis. (**D-F**) Microscopic images of human erythrocytes under different conditions: (**D**) in TBS buffer alone, (**E**) upon incubation for 60 min with 100 μg/mL DSP-3 and (**F**) pre-incubated with 100 μg/mL DSP-3 in presence of 20 mM PrC for 60 min. Scale bar = 5 μm.

23

In further studies aimed at investigating the effect of ligand binding to DSP-3 on its ability to induce erythrocyte lysis, the protein was pre-incubated with different concentrations of PrC, Lyso-PC, or choline chloride, which can block the phospholipid binding site of DSP-3 and prevent its binding to the choline phospholipids on the erythrocyte membrane. In these experiments it was observed that erythrocyte lysis was decreased in the presence of these choline-containing ligands (Fig. 9C), clearly indicating that DSP-3 induced destabilization is due to the binding of DSP-3 to the choline phospholipids present on the erythrocyte membrane. While 20 μM concentration of Lyso-PC could inhibit the erythrocyte lysis by >90%, similar inhibition was achieved by PrC and choline chloride only at 10 mM and 20 mM concentrations, respectively (Fig. 9C). Thus, these observations are consistent with the significantly higher association constant estimated for the binding of Lyso-PC to DSP-3 over PrC.

The erythrocyte membrane lysis induced by DSP-3 was also investigated by light microscopy using a confocal microscope. In these studies, images of human erythrocytes were taken in buffer and upon pre-incubation with DSP-3 alone as well as in the presence of ligands at different time intervals. Images of erythrocyte in buffer alone show well-defined morphology (Fig. 9D), whereas upon incubation with DSP-3 for 60 minutes, very few erythrocytes were seen together with some cell membrane fragments, indicating that the most of the erythrocyte were lysed and the cell membranes were fragmented (Fig. 9E). In samples where DSP-3 was pre-incubated with 20 mM PrC before adding to the sample, all erythrocytes were intact (Fig. 9F), indicating that binding of DSP-3 to choline phospholipids on the erythrocyte cell membrane inhibited the membrane destabilizing activity of the protein.

FnII proteins are the major macromolecules in the seminal plasma of various mammals and have been implicated in priming the spermatozoa for fertilization by inducing

cholesterol efflux from sperm plasma membranes, which is a crucial step in sperm *capacitation*. Therefore, the FnII proteins from the seminal plasma of various mammals have been isolated and purified and some of them have been characterized in considerable detail employing biochemical and biophysical approaches [24,52]. In particular, their interaction with model membranes containing choline phospholipids, which are their physiological ligands, as well as sperm plasma membranes and small molecules containing the choline moiety, such as choline and phosphoryl choline, were investigated by spectroscopic methods, isothermal titration calorimetry as well as other physical methods such as surface plasmon resonance [11,14,23,25,26,53]. The recent discovery that these proteins display chaperone-like activity (CLA) in a manner similar to small heat shock proteins (*shsp*s) led to increased interest in these proteins as they appear to be the only proteins in seminal plasma that exhibit the ability to protect other proteins against various kinds of stress conditions, viz., thermal, chemical and variation of pH [31-33]. In light of this, the present study reporting the purification and characterization of another major seminal FnII protein present in the donkey seminal plasma is quite significant. Further work to characterize the chaperone-like activity of DSP-3 is currently underway in our laboratory.

In summary, in the present work we have characterized DSP-3, another major protein from donkey seminal plasma in addition to DSP-1, belonging to the seminal FnII protein family and characterized its primary, secondary and tertiary structure by experimental and computational approaches. DSP-3 exhibits significantly higher homology to HSP-1 than DSP-1. It is a glycoprotein which is heterogeneously *O*-glycosylated and contains acetylated sialic acid residues. Differential scanning calorimetric studies have shown that DSP-3 unfolds in a two-state transition from a folded structure to the unfolded form and that ligand binding stabilizes the protein structure, and significantly increase in the transition temperature and enthalpy. Fluorescence titrations on the binding of PrC and Lyso-PC indicated that DSP-3

exhibits considerably higher binding affinity towards Lyso-PC than PrC. Additionally, the ability of DSP-3 to bind to choline phospholipids on cell membranes was investigated employing human erythrocytes as a model system, which showed that DSP-3 is capable of inducing membrane destabilization and can cause erythrocyte lysis. This would be physiologically quite relevant since similar activity on sperm cell membrane has been implicated in inducing acrosome reaction in spermatozoa which is a crucial step in sperm *capacitation* in various mammals [52]. Since the seminal FnII proteins have been found to exhibit multiple functional activities including chaperone like activity as *shsp*s, we propose to investigate the CLA of DSP-3 in future studies. Also, we propose to carry out further studies to investigate changes in the oligomeric status of the protein, if any, induced by its binding to the lipid membranes.

ACKNOWLEDGEMENTS

REFERENCES

[1]   C.R. Austin, The capacitation of mammalian sperm. Nature 170 (1952) 326. DOI: 10.1038/170326a0

[2]   M.C. Chang, The meaning of capacitation. A historical perspective, J. Androl. 5 (1984) 45-50. 10.1002/j.1939-4640.1984.tb00775.x

[3]   S. Shivaji, K.H. Scheit, P.M. Bhargava, Proteins of seminal plasma, Wiley, New York, 1990. ISBN-13: 978-0471846857

[4]   P.E. Visconti, H. Calantino-Hormer, G.D. Moore, J.L. Bailey, X. Ning, M. Fornes, G.S. Kopf, The molecular basis of sperm capacitation, J. Androl. 19 (1998) 242-248. DOI: 10.1002/j.1939-4640.1998.tb01994.x

[5]   R. Yanagimachi, Mammalian fertilization in: E. Knobil, J. Neill (Eds.), Physiology of Reproduction, Raven Press, New York, (1994) pp. 189-317. CRID-1571135651032479488

[6]   R.A.P. Harrison, Capacitation mechanisms and the role of capacitation as seen in eutherian mammals, Reprod. Fertil. Dev. 8 (1996) 581-596. DOI: 10.1071/rd9960581

[7]   T.M. Gwathmey, G.G. Ignotz, S.S. Suarez, PDC-109(BSP-A1/A2) promotes bull sperm binding to oviductal epithelium in vitro and may be involved in forming the oviductal sperm reservoir, Biol. Reprod. 69 (2003) 809–815. DOI: 10.1095/biolreprod.102.010827

[8]   F.S. Esch, N.C. Ling, P. Bohlen, S.Y. Ying, R. Guillemin, Primary structure of PDC-109, a major protein constituent of bovine seminal plasma, Biochem. Biophys. Res. Commun. 113 (1983) 861–867. DOI: 10.1016/0006-291x(83)91078-1

[9]   N.G. Seidah, P. Manjunath, J. Rochemont, M.R. Sairam, M. Chrétien, Complete amino acid sequence of BSP-A3 from bovine seminal plasma. Homology to PDC-109 and to

the collagen-binding domain of fibronectin, Biochem J 243 (1987) 195-203. DOI: 10.1042/bj2430195

[10] L. Desnoyers, and P. Manjunath, Major proteins of bovine seminal plasma exhibit novel interactions with phospholipids, J. Biol. Chem. 267 (1992) 10149-10155. PMID: 1577785

[11] M. Ramakrishnan, V. Anbazhagan, T.V. Pratap, D. Marsh, M.J. Swamy, Membrane insertion and lipid-protein interactions of bovine seminal plasma protein PDC-109 investigated by spin-label electron spin resonance spectroscopy, Biophys. J. 81 (2001) 2215-2225. DOI: 10.1016/S0006-3495(01)75869-9

[12] A. Greube, K. Müller, E. Töpfer-Petersen, A. Herrmann, P. Müller, Interaction of Fn type II proteins with membranes: stallion seminal plasma protein SP-1/2, Biochemistry 43 (2004) 464-472. DOI: 10.1021/bi035547l

[13] J. Fan, J. Lefebvre, P. Manjunath, Bovine seminal plasma proteins and their relatives: a new expanding super family in mammals, Gene 375 (2006) 63–74. DOI: 10.1016/j.gene.2006.02.023

[14] M.J. Swamy, D. Marsh, V. Anbazhagan, M. Ramakrishnan, Effect of cholesterol on the interaction of seminal plasma protein, PDC-109 with phosphatidylcholine membranes, FEBS Lett. 528 (2002) 230-234. DOI: 10.1016/S0014-5793(02)03316-1

[15] P. Müller, A. Greube, E. Töpfer-Petersen, A. Herrmann, Influence of the bovine seminal plasma protein PDC-109 on cholesterol in the presence of phospholipids, Eur. Biophys. J. 31 (2002) 438-447. DOI: 10.1007/s00249-002-0234-2

[16] S. Scolari, K. Müller, R. Bittman, A. Hermann, O. Müller, Interaction of mammalian seminal plasma protein, PDC-109 with cholesterol: implications for a putative CRAC domain. Biochemistry 49 (2010) 9027-9031. DOI: 10.1021/bi101257c

[17] A. Romero, P.F. Varela, E. Topfer-Petersen, J.J. Calvete, Crystallization and preliminary X-ray diffraction analysis of bovine seminal plasma PDC-109, a protein composed of two fibronectin type II domains. Proteins 28 (1997) 454-456. DOI: 10.1002/(sici)1097-0134(199707)28:3<454::aid-prot14>3.0.co;2-g

[18] D.A. Wah, C. Fernández-Tornero, L. Sanz, A. Romero, J.J. Calvete, Sperm coating mechanism from the 1.8 Å crystal structure of PDC-109-phosphorylcholine complex, Structure 10 (2002) 505-514. DOI: 10.1016/s0969-2126(02)00751-7

[19] J.J. Calvete, S. Nessau, K. Mann, L. Sanz, H. Sieme, L. Klug, E. Töpfer-Petersen, Isolation and biochemical characterization of stallion seminal plasma proteins, Reprod. Domest. Anim. 29 (1994) 411-426. DOI: 10.1111/j.1439-0531.1994.tb00588.x

[20] J.J. Calvete, K.H. Mann, W. Schafer, L. Sanz, M. Reinert, S. Nessau, E. Töpfer-Petersen, Amino acid sequence of HSP-1, a major protein of stallion seminal plasma: effect of glycosylation on its heparin and gelatin-binding capabilities, Biochem. J. 310 (1995) 615-622. DOI: 10.1042/bj3100615

[21] J.J. Calvete, M. Reinert, L. Sanz, E. Töpfer-Petersen, Effect of glycosylation on the heparin-binding capability of boar and stallion seminal plasma proteins, J. Chromatogr. A 711 (1995) 167-173. DOI: 10.1016/0021-9673(95)00011-b

[22] A. Tannert, A. Kurz, K. R.Erlemann, K. Müller, A. Herrmann, J. Schille, E. Töpfer-Petersen, P. Manjunath, P. Müller, The bovine seminal plasma protein PDC-109 extracts phosphorylcholine-containing lipids from the outer membrane leaflet, Eur. Biophys. J. 36 (2007) 461-475. DOI: 10.1007/s00249-006-0105-3

[23] V. Anbazhagan, M. J. Swamy, Thermodynamics of phosphorylcholine and lysophosphatidylcholine binding to the major protein of bovine seminal plasma, PDC-109, FEBS Lett. 579 (2005) 2933-2938. DOI: 10.1016/j.febslet.2005.04.046

[24] M.J. Swamy, Interaction of bovine seminal plasma proteins with model membranes and sperm plasma membranes, Curr. Sci. 87 (2004) 203-212. https://www.jstor.org/stable/24108866

[25] P. Müller, K.-R. Erlemann, K. Müller, J. J. Calvete, E. Topfer-Petersen, K. Marienfeld, A. Herrmann, Biophysical characterization of the interaction of bovine seminal plasma protein PDC-109 with phospholipid vesicles, Eur. Biophys. J. 27 (1998) 33– 41. DOI: 10.1007/s002490050108

[26] M. Gasset, L. Magdaleno, J.J. Calvete, Biophysical study of the perturbation of model membrane structure caused by seminal plasma protein PDC-109, Arch. Biochem. Biophys. 374 (2000) 241-247. DOI: 10.1006/abbi.1999.1593

[27] V. Anbazhagan, R.S. Sankhala, B.P. Singh, M.J. Swamy, Isothermal titration calorimetric studies on the interaction of the major bovine seminal plasma protein, PDC-109 with phospholipid membranes, PLoS ONE 6 (2011) e25993. DOI: 10.1371/journal.pone.0025993

[28] R.S. Damai, R.S. Sankhala, V. Anbazhagan, M.J. Swamy, ^{31}P-NMR and AFM studies on the destabilization of cell and model membranes by the major bovine seminal plasma protein, PDC-109, IUBMB Life 62 (2010) 841-851. DOI: 10.1002/iub.394

[29] C.S. Kumar, M.J. Swamy, A pH switch regulates the inverse relationship between membranolytic and chaperone-like activities of HSP-1/2, a major protein of horse seminal plasma, Biochemistry 55 (2016) 3650-3657. DOI: 10.1021/acs.biochem.5b01374

[30] S. Alim, C.S. Kumar, M. Laitaoja, T. R. Talluri, J. Jänis, M. J. Swamy, Purification, molecular characterization and ligand binding properties of the major donkey seminal plasma protein DSP-1, Int. J. Biol. Macromol. 194 (2022) 213-222. DOI: 10.1016/j.ijbiomac.2021.11.177

[31] R.S. Sankhala, M. J. Swamy, The major protein of bovine seminal plasma, PDC-109 is a molecular chaperone, Biochemistry 49 (2010) 3908-3918. DOI: 10.1021/bi100051d

[32] R.S. Sankhala, C.S. Kumar, B.P. Singh, A. Arangasamy, M.J. Swamy, HSP-1/2, a major protein of equine seminal plasma, exhibits chaperone-like activity, Biochem. Biophys. Res. Commun. 427 (2012) 18–23. DOI: 10.1016/j.bbrc.2012.08.120

[33] C.S. Kumar, M.J. Swamy, HSP-1/2, a major horse seminal plasma protein, acts as a chaperone against oxidative stress, Biochem. Biophys. Res. Commun. 473 (2016)1058–1063. DOI: 10.1016/j.bbrc.2016.04.015

[34] R.S. Sankhala, R.S. Damai, M.J. Swamy, Correlation of membrane binding and hydrophobicity to the chaperone-like activity of PDC-109, PLoS ONE 6 (2011) e17330. DOI: 10.1371/journal.pone.0017330

[35] C.S. Kumar, B. P. Singh, S. Alim, M.J. Swamy, Factors influencing the chaperone-like activity of major proteins of mammalian seminal plasma, equine HSP-1/2 and bovine PDC-109: Effect of membrane binding, pH and ionic strength, Adv. Exp. Med. Biol. 5 (2018) 53-68. DOI: 10.1007/978-981-13-3065-0_5

[36] B. P. Singh, A. Asthana, A. Basu, T. Ramakrishna, Ch. M. Rao, M. J. Swamy, Conserved core tryptophans of FnII domains are crucial for the membranolytic and chaperone-like activities of bovine seminal plasma protein, PDC-109, FEBS Lett. 594 (2020) 509-518. DOI: 10.1002/1873-3468.13617

[37] B. P. Singh, R. S. Sankhala, A. Asthana, T. Ramakrishna, Ch. M. Rao, M. J. Swamy, Glycosylation differentially modulates membranolytic and chaperone-like activities of PDC-109, the major protein of bovine seminal plasma, Biochem. Biophys. Res. Commun. 511 (2019) 28-34. DOI: 10.1016/j.bbrc.2019.02.002

[38] S. Alim, S. Das, M.J. Swamy, Probing the chemical unfolding and phospholipid binding to the major protein of donkey seminal plasma, DSP-1 by fluorescence

spectroscopy, J. Photochem. Photobiol. A: Chem. 440 (2023) Art. No. 114643. DOI: 10.1016/j.jphotochem.2023.114643

[39] U.K. Laemmli, Cleavage of structural proteins during the assembly of the head of bacteriophage T4, Nature 227 (1970) 680-685. DOI: 10.1038/227680a0

[40] S. Mondal, M.J. Swamy, Purification, biochemical/biophysical characterization and chitooligosaccharide binding to BGL24, a new PP2-type phloem exudate lectin from bottle gourd (*Lagenaria siceraria*), Int. J. Biol. Macromol. 164 (2020) 3656-3666. DOI: 10.1016/j.ijbiomac.2020.08.246

[41] J.J. Calvete, K. Mann, L. Sanz, M. Raida, E. Töpfer Petersen, The primary structure of BSP-30K, a major lipid-, gelatin- and heparin binding glycoprotein of bovine seminal plasma, FEBS Lett. 399 (1996) 147-152. DOI: 10.1016/s0014-5793(96)01310-5

[42] P.S. Jois, P. Manjunath, The N-terminal part of Binder of SPerm 5 (BSP5), which promotes sperm capacitation in bovine species is intrinsically disordered, Biochem. Biophys. Res. Commun. 394 (2010) 1036-1041. DOI: 10.1016/j.bbrc.2010.03.118

[43] M. Gasset, J.L. Saiz, L. Sanz, M. Gentzel, E. Töpfer-Petersen and J.J. Calvete, Conformational features and thermal stability of bovine seminal plasma protein PDC-109 oligomers and phosphoryl choline bound complexes, Eur. J. Biochem. 250 (1997) 735-744. DOI: 10.1111/j.1432-1033.1997.00735.x

[44] A.S. Mahadevi, G.N. Sastry, Cation−π interaction: Its role and relevance in chemistry, biology, and material science, Chem. Rev. 113 (2013) 2100-2138. DOI: 10.1021/cr300222d

[45] S. Horowitz, R.C. Trievel, Carbon-oxygen hydrogen bonding in biological structure and function, J. Biol. Chem. 287 (2012) 41576-41582. DOI: 10.1074/jbc.r112.418574

[46] M. Brandl, M.S. Weiss, A. Jabs, J. Sühnel, R. Hilgenfeld, C-H···π-interactions in proteins, J. Mol. Biol. 307 (2001) 357-377. DOI: 10.1006/jmbi.2000.4473

[47] D.M. Chipman, V. Grisaro, N. Sharon, binding of oligosaccharides containing *N*-acetylglucosamine and *N*-acetylmuramic acid to lysozyme: the specificity of binding subsites, J. Biol. Chem. 242 (1967) 4388-4394. DOI: 10.1016/S0021-9258(18)99551-7

[48] T. Mann, C. Lutwak-Mann, Male Reproductive Function and Semen, Springer-Verlag, Berlin, 1981. ISBN: 978-1-4471-1300-3

[49] W.V. Holt, R.D. North, Determination of lipid composition and thermal phase transition temperature in an enriched plasma membrane fraction from ram spermatozoa, J. Reprod. Fertil. 73 (1985) 285-294. DOI: 10.1530/jrf.0.0730285

[50] J.E. Parks, J.A. Arion, R.H. Foote, Lipids of plasma membrane and outer acrosomal membrane from bovine spermatozoa, Biol. Reprod. 37 (1987) 1249-1258. DOI: 10.1095/biolreprod37.5.1249

[51] P. Martínez, A. Morros, Membrane lipid dynamics during human sperm capacitation, Front. Biosci. 1 (1996) 103-117. DOI: 10.2741/a119

[52] G. Plante, B. Prud'homme, J. Fan, M. Lafleur, P. Manjunath, Evolution and function of mammalian binder of sperm protein, Cell Tissue Res. 363 (2016) 105-127. DOI: 10.1007/s00441-015-2289-2

[53] C.J. Thomas, V. Anbazhagan, M. Ramakrishnan, N. Sultan, I. Surolia, M.J. Swamy, Mechanism of membrane binding by the bovine seminal plasma protein, PDC-109. A surface plasmon resonance study, Biophys. J. 84 (2003) 3037-3044. DOI: 10.1016/S0006-3495(03)70029-0

AUTHOR STATEMENT

Sk Alim: Data curation; Formal analysis; Investigation; Methodology; Writing – review & editing

Mikko Laitaoja: Data curation; Formal analysis; Writing – original draft

Sonali S. Pawar: Investigation; Methodology

Thirumala Rao Talluri: Methodology - sample collection and processing

Janne Jänis: Resources; Supervision - mass spectrometric studies; Funding acquisition; Writing – review & editing

Musti J. Swamy: Conceptualization; Funding aquisition; Project administration; Resources; Supervision; Writing – review & editing

Declaration of interests

☐The authors declare that they have no known competing financial interests or personal relationships that could have appeared to influence the work reported in this paper.

☒The authors declare the following financial interests/personal relationships which may be considered as potential competing interests:

HIGHLIGHTS

- Another FnII protein from donkey seminal plasma, DSP-3 was purified and characterized

- DSP-3 exhibits higher homology to equine HSP-1 than donkey FnII protein DSP-1

- High-resolution LC-MS analysis indicated that DSP-3 is heterogeneously *O*-glycosylated

- DSP-3 unfolds at ~45°C and phosphorylcholine binding stabilizes its structure considerably

- DSP-3 perturbs erythrocyte membranes by specifically binding to choline phospholipids